Assessment and Enhancement of FRC of Power Systems Considering Thermal Power Dynamic Conditions

Feng Hong, *Member*, *IEEE*, *Member*, *CSEE*, Yalei Pang, Weiming Ji, Lu Liang, Fang Fang *Senior Member*, *IEEE*, *Senior Member*, *CSEE*, Junhong Hao, *Member*, *IEEE*, *Member*, *CSEE*, and Jizhen Liu, *Fellow*, *CSEE*

***Abstract*—Frequency stability and security have been a vital challenge as large-scale renewable energy is integrated into power systems. In contrast, the proportion of traditional thermal power units decreases during the decarbonization transformation process, resulting in poor frequency support. This paper aims to explore the potential of frequency regulation support, dynamic assessment, and capacity promotion of thermal power plants in the transition period. Considering the dynamic characteristics of the main steam working fluid under different working conditions, a nonlinear observer is constructed by extracting the main steam pressure and valve opening degree parameters. The real-time frequency modulation capacity of thermal power units can provide a dynamic state for the power grid. A dynamic adaptive modification for primary frequency control (PFC) of power systems, including wind power and thermal power, is proposed and improved. The power dynamic allocation factor is adaptively optimized by predicting the speed droop ratio, and the frequency modulation capability of the system is improved by more than 11% under extreme conditions. Finally, through the Monte Carlo simulation of unit states of the system under various working conditions, the promotion of the frequency regulation capacity with high wind power penetration (WPP) is verified.**

***Index Terms*—Dynamic evaluation, frequency regulation, power system, predictive modeling, wind penetration.**

I. Introduction

THE global growth of photovoltaic, wind, and other renewable energy generation has gained booming development, and the installed capacity of renewable power generation has been rising for decades [1], [2]. To achieve sustainable development of energy, economy, and society, the "dual carbon" targets have been proposed and adopted as one of the essential national strategies in China [3], [4]. Power systems are undergoing a transition period during which the main generation sources change from large-scale integrated coal-fired units to intermittent renewable energy sources [5], [6]. The security and stability of power systems are challenged more seriously with the transformation of the generation side. Frequency is one of the most critical indicators in evaluating the power system's security and power balance [7], [8]. Ensuring frequency stability is the premise of realizing the value of the power grid [9], [10]. With the further expansion of the installed renewable energy and the decline of the proportion of installed conventional thermal power, the frequency stability of the power system has been tremendously challenged [11], [12]. On the one hand, the inertial support based on thermal power has changed, resulting in scarce frequency modulation resources and reduced frequency modulation margin [13]. On the other hand, the stochastic of renewable energy increases the complexity of the working conditions of thermal power units and further leads to the shrinking of frequency regulation capacity [14].

In China, thermal power plants play the predominant role in frequency regulation during the transitional period of power systems [15]. Therefore, these coal-fired power units will need more frequency modulation tasks for an extended period [16]. For example, the power plants in North China and Northwest China have been operating at low loads (loads less than 50%) for a long time [17]. The thermal power unit in this situation will harm the frequency security of the power system. Therefore, improving the frequency regulation capability (FRC) of thermal power plants is inevitable for the new power grid. Wang *et al*. [18] proposed a nonlinear algorithm to improve the economy of flexible retrofit of thermal power units. Hentschel *et al*. [19] modeled a coal-fired power plant in detail through Apros to realize the dynamic simulation of thermal power output. Han *et al*. [20] proposed load optimization scheduling thermal units during grid operation. The key to the control is to adjust the load command to a load range with better regulation performance (60%–90% Rated load). The above studies have proved that thermal power flexibility transformation is widely promoted. However, the dynamic characteristics of the units at the flexibility modification show a tremendous difference, with deep peak shaving leading to more pronounced changes. Much of the existing research has focused on power system flexibility influenced by different load ranges of thermal power plants. Many studies on thermal power generation regulation characteristics under dynamic operating conditions are still

Manuscript received June 28, 2023; revised August 8, 2023; accepted September 5, 2023. Date of online publication May 3, 2024; date of current version June 20, 2023. This work was supported by the Science and Technology Project of State Grid Corporation of China (52060021N00P).

F. Hong, Y. L. Pang, W. M. Ji, L. Liang, F. Fang and J. Z. Liu are with the State Key Laboratory of Alternate Electric Power System with Renewable Energy Sources and School of Control and Computer Engineering, North China Electric Power University, Beijing 102206, China.

J. H. Hao (corresponding author, email: hjh@ncepu.edu.cn) is with the State Key Laboratory of Alternate Electric Power System with Renewable Energy Sources, School of Energy Power and Mechanical Engineering, North China Electric Power University, Beijing 102206, China.

DOI: 10.17775/CSEEJPES.2023.04990

inadequate. It is generally considered that the primary frequency modulation (PFM) of the system focuses on inertia support [21]. Fig. 1 shows the PFM, which includes the inertia support and the generator output response. In the conventional PFM, the influence of the steam turbine side on frequency modulation is mainly considered, and the storage state of the boiler side is ignored [22]. It is worth noting that continuous frequency modulation when the unit is operating at a low load can lead to a decrease in storage capacity, which makes the frequency modulation capacity decrease rapidly and thus affects the unit's peaking and frequency modulation capacity. Therefore, it is necessary to study the frequency modulation capacity of the unit under dynamic conditions to improve the utilization efficiency of frequency modulation resources.

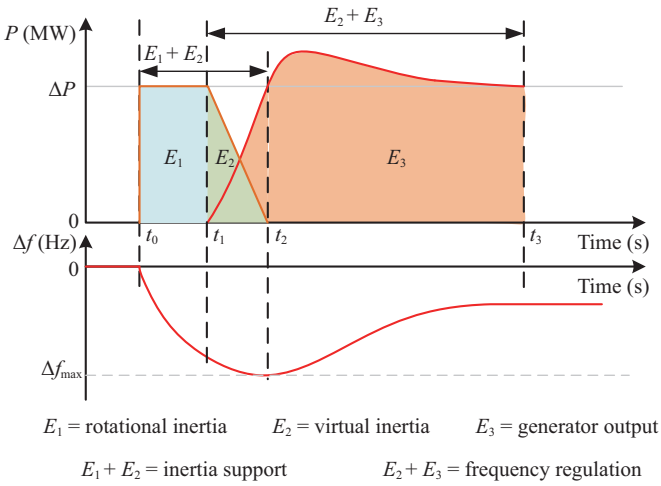

Fig. 1. Unit response to primary frequency modulation.

As an important part of new energy, wind power generation (WG) has the characteristics of being pollution-free and renewable, so it has become an essential part of developing a modern power system [23], [24]. However, its ability to participate in grid frequency modulation is poor due to the randomness and intermittence of WG [25]. Many countries have stipulated requirements for improving power system frequency stability with increasing grid-connected WPP [26], [27]. When the frequency modulation command comes, WG needs to provide certain frequency support to enhance the frequency modulation performance of the power grid [28]. Yao *et al*. [29] proposed a frequency regulation strategy for wind power systems using fuzzy proportional–derivative (PD) control, which effectively improved the frequency stability of the grid. Abazari *et al*. [30], [31] verified that the frequency support to the power system would be enhanced when more WG is integrated into the power system. However, the frequency modulation capability of wind turbines has certain limitations due to its characteristics in the current research. Meanwhile, the increased penetration of wind power will affect the operation of thermal power, and the system's thermal units will often drop into low-load areas [32], [33]. The two points lead to the compression of the overall frequency modulation capability of the power system. In addition, the randomness and uncertainty of wind power also make thermal power more frequent, which increases the difference in thermal power dynamic conditions.

High WPP leads to the instability of thermal power frequency regulation capacity, so it is urgent to establish a more refined PFC evaluation model for power systems [34]. Whether the active power balance can be achieved is the key to the evaluation of power system capacity. Conventionally, there are two kinds of PFC evaluation: behavior and capacity evaluation. The behavior evaluation is a lagging estimation, which is realized by reward and punishment after the change of response frequency difference of the power system [35], [36]. The capacity evaluation pays more attention to the upper and lower limits of frequency deviation response under different working conditions [37]. Gao *et al*. [38] proposed an online estimation algorithm for PFM characteristic parameters of grid-connected operating units through real-time data processing of power grids. Liao [39] conducted standard training and test data on the turbine-boiler coordinated control system and digital electric-hydraulic control system coupling model, and designed a neural network to evaluate the PFM response ability of the unit. Recently, there have still been few studies on unit performance evaluation and no dynamic evaluation considering the current state of thermal power units.

At present, with the increasing dynamic differences, it is an urgent problem to tap the potential of flexible resources to maximize the utilization of frequency modulation. This paper considers the frequency regulation characteristics of power systems under high WPPs. In view of the need for refined evaluation of power systems under dynamic differences and the need for greater utilization of frequency modulation resources, the following innovations are proposed in the study of the frequency regulation capacity of conventional systems.

1) A nonlinear full-state observation model considering the real-time state of a thermal power unit is proposed, and the primary frequency regulation capacity of the unit can be dynamically evaluated by the main steam pressure and the valve opening degree.

2) A dynamic adaptive modification for primary frequency control of power systems is proposed. The unit coordination is achieved by dynamically adjusting the adaptive optimization of the dynamic power allocation factor through the predicted speed droop ratio.

Other parts of this paper are as follows. Section II introduces the overall model of the proposed system. An improved control strategy is proposed in Section III. In Section IV, simulation and verification are carried out. Finally, Section V presents some conclusions.

II. The Overall Model of The Power System

The power system is a complex dynamic system. PFM plays an essential role in the modern power system and is a dynamic means to ensure the grid's active power balance by adjusting the grid frequency variation and keeping the grid frequency stable. Fig. 2 shows the overall layout of the PFC in the modern power system studied in this paper. Wherein the system consists of ten thermal power units (with a capacity of 315 MW) with combined frequency regulation in different

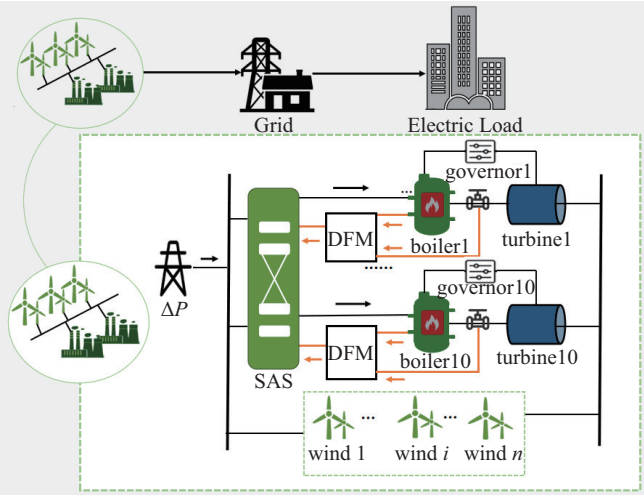

Fig. 2. General layout of the PFC in the power grid.

states and n wind power systems. Thermal and wind power are jointly coordinated to form the total output to the grid. In the PFM, the load side disturbance (ΔP) is transformed into frequency difference input to the Self-adjusting system (SAS) through the grid and then allocated to each thermal power plant after adjustment. Among them, DFM is an output dynamic forecasting module. Each unit can adjust the output by dynamically predicting the return state. The frequency deviation determines the output power of WG. Assuming n wind turbines, WPP is only related to the number of turbines.

A. Thermal Power in Modern Power System

Due to the large-scale integration of WG, thermal power is currently facing an increasingly severe challenge in China. Dynamic performance is essential for thermal power participation in primary frequency regulation. Various flexible transformation technologies have been proposed, but the influence of state parameters on the boiler side is generally not considered in the frequency modulation process. Most of the previous studies have concluded that the state of the turbine mainly determines the dynamic frequency characteristics of thermal power units. The influence of boiler-side parameters directly determines the energy storage of the unit, which affects the PFC performance of the unit. Therefore, the boiler side needs to be considered when modeling the frequency regulation of the unit.

In this paper, the ten thermal power units introduced are of the same type, in which the boiler model adopts the simplified nonlinear model of the steam-laden furnace unit proposed by our team [40]. The model can reflect the dynamic characteristics of the steam-laden furnace units and has certain generality. The dynamic transfer function model of the coal mill and the water-cooled wall is as follows:

$$G_m(s) = \frac{-1}{(30s+1)(5s+1)} \mathrm{e}^{-40s} \tag{1}$$

The boiler core state space model is given in the following equations:

$$\begin{cases} p_b = -0.0389(p_b - p_t)^{0.5} + 0.0463 D_q \\ p_t = 0.7(p_b - p_t)^{0.5} - 0.0476 p_t u_t \\ D_t = 60 p_t u_t \end{cases} \tag{2}$$

where p_b is the drum pressure, MPa. D_q is the effective heat absorption of a standard boiler. p_t indicates primary steam pressure, MPa. D_t represents the main steam flow rate, t/h. u_t is valve opening degree, %.

Figure 3(a) shows the conventional non-decoupled model mainly used. The overshoot phenomenon influenced by intermediate reheat volume is characterized by the introduction of the high-pressure cylinder overshoot coefficient according to the improved dynamic theory model proposed in China. The turbine simulation model is established as shown in Fig. 3(b). $F_{i\mathrm{P}}$ is the power factor of a specific cylinder. $T_{i\mathrm{P}}$ is the time constant of steam flowing through the pipe.

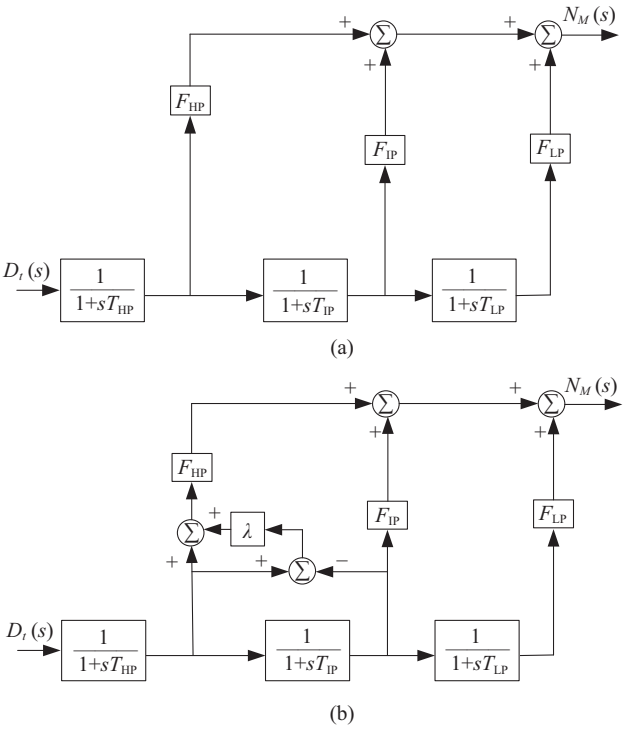

Fig. 3. Dynamic model of reheat steam turbine. (a) Non-decoupling turbine model. (b) Single decoupling turbine model.

Neglecting the steam volume effect parameter of the connecting tube between the medium and low-pressure cylinders, the model in Fig. 3(b) can be derived as:

$$\frac{N_M(s)}{D_t(s)} = \frac{1 + s\lambda T_{\mathrm{IP}} F_{\mathrm{HP}} + s T_{\mathrm{IP}} F_{\mathrm{HP}}}{(1+sT_{\mathrm{HP}})(1+sT_{\mathrm{IP}})} \tag{3}$$

B. Wind Power Model in Modern Power System

As the main force among the new energy turbines, wind turbines will be studied in this paper as their representatives. In this paper, inertia control is used to describehe way wind turbines provide virtual inertia support [41]. The output of wind turbine to the disturbance caused by frequency difference is as follows:

$$\Delta P_{\mathrm{NC}}(s)=\frac{sT_\omega\times\Delta f}{R_{\mathrm{wind}}(1+sT_r)(1+sT_\omega)\left[\left(K_{\omega p}+\frac{K_{\omega i}}{s}\right)\frac{1}{2sH_{\mathrm{e}}}-(sT_a+1)\right]} \tag{4}$$

where s is the Laplacian operator, and H_{e} is the equivalent wind unit inertia. Δf would pass through frequency measurement $1/(1+sT_r)$, washout filter $1/(1+sT_\omega)$, and a proportional gain $1/R_{\mathrm{wind}}$ to produce a transient and fast power. R_{wind} is the droop constant of WG, which describes the maximum regulation power provided by the WG. The symbol indicates the ability of the WG to support frequency deviations. After the release of kinetic energy, the rotor speed will be recovered by the PI controller $(K_{wp}+K_{wi}/s)$.

Currently, the model of the generator is uncontroversial and simplified to $1/(2Hs+D)$. D is the load-damping constant. H is the inertia constant of the power system. The inertia constant H of the equivalent generator is equal to the sum of the inertia constants of all generator sets, independent of the output power and frequency $H=\sum_m H_j$.

C. The Performances of PFC in Different States

Performing PFC dynamic evaluation under flexibility is necessary for thermal power-generating units. The previous AGC response condition determines the dynamic working condition, and the amount of heat storage has a decisive influence on the PFC. For a single unit, there is a deviation between the command and the active power if the unit has insufficient heat storage (as shown in Fig. 4). However, the shaded area in Fig. 4 is energy deficient. Hence, the unit energy response is insufficient for the PFC command. In this case, the output energy of the original instruction can't meet the demand, and the unit needs an additional energy supplement to complete the command.

Meanwhile, units operating at low loads have different regulation characteristics than those operating at high loads. For example, the deep peak shaving of conventional units means that as the WPP increases or decreases, the conventional unit adjusts its output to fit the output of the WG. Operating during deep peak shaving means that it faces frequent start-up and large-scale load changes, and the working conditions are more complicated. As a result, the heat storage utilization process in the generator set is more limited. This puts forward new requirements for units, as the thermal intensity of the boiler chamber is too low to adapt to changing operating conditions. With flexible modifications, coal-fired plants can operate at 30% or 35%–100% of the rated load. With the massive grid integration of wind power, units operating at deep peak shaving conditions are becoming more common. When the unit is in an extreme situation, such as multiple successive PFMs under deep peak shaving, the actual response to the PFC instruction will be much lower than the PFC instruction, as shown in Fig. 4(b). In general cases, there is only a small gap between the actual response and the unit instruction. In extreme cases, the unit cannot provide enough energy, and there will be a large shortage of energy. This is a typical case of suboptimal PFC performance.

For the whole system, the presence of multiple units allows the entire system to coordinate and thus adjust the PFC output. The prediction model presented in Section III-A is used to predict the real-time status of each unit, and a strategy is designed in Section III-B to utilize each unit's energy storage fully.

III. Modeling and Analysis of System Considering Thermal Power Dynamic State

A. PFC Prediction Model Considering Dynamic Processes

When the generator speed deviates from 3 000 r/min, the power system starts PFC. The heat storage of the boiler is used to respond to Δn (value shift). The boiler's storage state determines the unit's PFM response rate and capability. During actual operation (as shown in Fig. 5), a large amount of stored energy is stored in the steam and water work and work piping on the boiler side of the unit, and the release of this stored

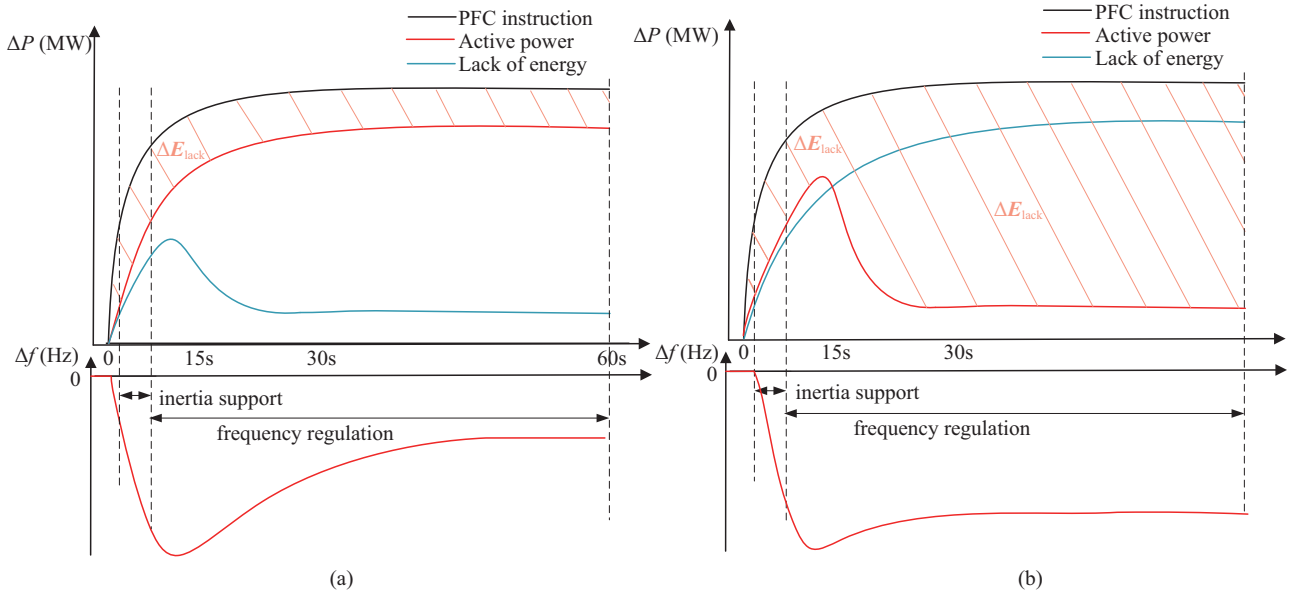

Fig. 4. PFC different state response process. (a) General state. (b) Extreme state.

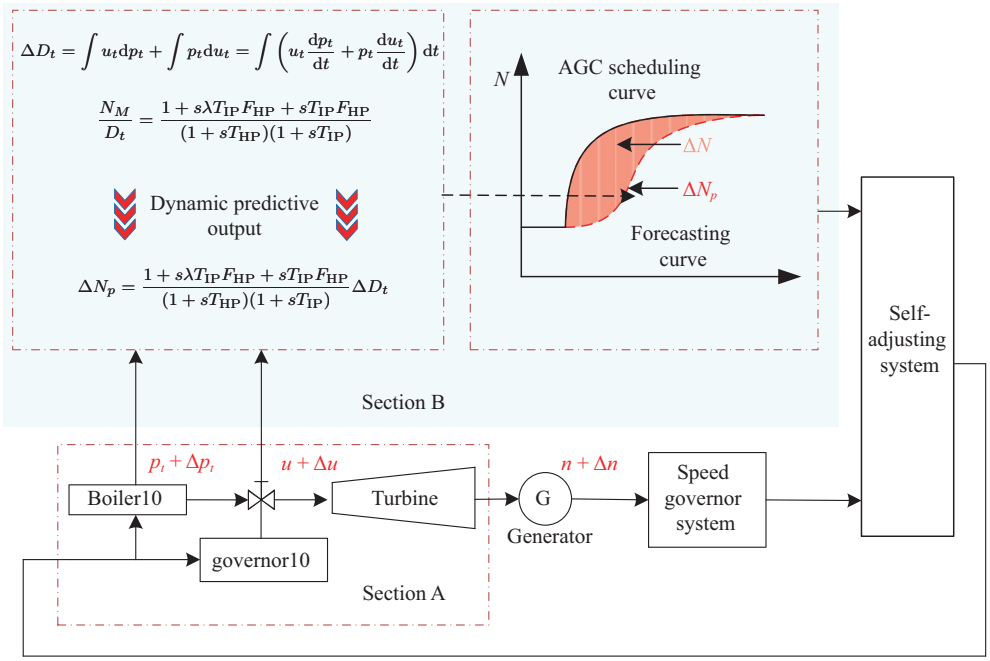

Fig. 5. General layout of a single thermal power unit.

energy depends on the change of valve opening degree. At the beginning of PFC, the steam intake to the turbine can be adjusted by changing the valve opening degree, thus making full use of the stored energy on the boiler side of the unit. The main steam pressure and the valve opening degree are essential factors affecting the PFC capacity. Due to the unstable state of boiler energy storage, dynamic prediction and evaluation of the unit's real-time FRC are also required. The difference between the predicted power output and the required power output is designed as a control strategy to change the actual power output.

Section A describes the thermal unit coordinated control section in Fig. 5, and Section B describes the dynamic prediction model based on nonlinear full-state observations.

The controlled object of the unitary coordinated control system is a complex multivariable system with strong coupling characteristics. The dynamic model structure of the system reflects the relationship between the components on the one hand and the essential nonlinear characteristics of the system on the other.

The energy relationship between the components is as follows:

1) The ladle pressure (p_b) reflects the relationship between the amount of heat absorbed by the boiler (D_q) and the amount of steam generated at the ladle outlet (D_k), and the ladle heat storage coefficient (C_d) reflects the amount of energy stored in the ladle.

2) The main steam pressure (p_t) reflects the relationship between the amount of steam generated at the ladle outlet (D_k) and the amount of steam generated at the main steam (D_t). The heat storage coefficient (C_t) reflects the energy stored in the main steam piping.

Considering the energy storage of the boiler ladle, the first energy relationship equation is obtained as follows:

$$\Delta D_q - \Delta D_k = C_d \frac{\mathrm{d}\Delta p_b}{\mathrm{d}t} \tag{5}$$

Considering the energy storage in the main steam pipe, the second energy relationship equation can be obtained:

$$\Delta D_k - \Delta D_t = C_t \frac{\mathrm{d}\Delta p_t}{\mathrm{d}t} \tag{6}$$

The non-linear dynamic nature is reflected in two main aspects:

1) The square root relationship between the pressure drop of the ladle pressure and the main steam pressure and the steam flow rate at the ladle outlet.

2) The main steam flow rate is equal to the product of the valve opening degree (u_t) and the main steam pressure.

The following two equations can describe them:

$$p_b - p_t = k D_k^2 \tag{7}$$

$$D_t = \mu_t \times P_t \tag{8}$$

The PFM output dynamic prediction model is crucial to predicting the dynamic output. Parameters which are p_t and u_t are essential factors that affect the PFC capacity. The main steam flow rate into the turbine work is changed by changing the valve opening degree, thus changing the unit output. Since the unit output is correlated with the main steam flow, the change in unit output is derived by predicting the amount of change in the unit's main steam flow to predict the unit's output increment at the current moment.

During the whole dynamic process, the state of the boiler and the steam turbine jointly determine the main steam pressure and main steam flow. Usually, the output is determined by two components: the energy contribution from the fuel-side input of the boiler and the effect of the change in the turbine valve opening degree. For PFC, the fuel-side factor leads to a limited impact on the unit's FRC so that the fuel-side fluctuations can be ignored.

For the main steam flow model, by taking differentiation on both sides of (8), we obtain.

$$\mathrm{d}\Delta D_t = u_t \mathrm{d}p_t + p_t \mathrm{d}u_t \tag{9}$$

Taking the integral of both sides of the equation:

$$\Delta D_t = \int u_t \mathrm{d}p_t + \int p_t \mathrm{d}u_t = \int \left(u_t \frac{\mathrm{d}p_t}{\mathrm{d}t} + p_t \frac{\mathrm{d}u_t}{\mathrm{d}t} \right) \mathrm{d}t \tag{10}$$

The main steam flow determines turbine operation, and the incremental prediction model of the output can be deduced from (3):

$$\Delta N_p = \frac{1 + s\lambda T_{\mathrm{IP}} F_{\mathrm{HP}} + s T_{\mathrm{IP}} F_{\mathrm{HP}}}{(1 + s T_{\mathrm{HP}})(1 + s T_{\mathrm{IP}})} \Delta D_t \tag{11}$$

The above derivation provides the main steam flow prediction model and turbine output power. Therefore, the unit frequency modulation output can be evaluated in real time.

B. Improved Coordination Control Strategy

The prediction model proposed in Section III allows for dynamic prediction of the PFC output. The fluctuations of the units can increase and change dramatically throughout the system operation, especially under low load conditions, so there is an urgent need for prior assessment to ensure the grid's security.

The speed droop ratio δ is the ratio of the normalized frequency deviation to the normalized variation of the generated power, and it is usually considered the most critical performance indicator of the PFC. Power factor correction experiments have yielded a speed droop ratio, usually between 4% and 6%, which is reasonable. A low-speed droop ratio implies a strong power factor correction capability. The speed droop ratio belongs to the post-evaluation of the grid to master the regional frequency security margin through experiments. However, the post-evaluation is not helpful for the unit to perform the regulation of FRC, so it is necessary to evaluate it in advance. The model proposed in this paper can predict the unit speed droop ratio and evaluate the PFC capability of the units to design a strategy to self-adjust the unequal speed rate of each unit in the system, improve the unit FRC, and enhance the grid security.

The accuracy of the prediction model has been verified in Section III, so that the predicted speed droop ratio can be calculated as follows:

$$\delta_{\mathrm{pred}} = \frac{\Delta x / x_0}{\Delta y / P_0} \% \tag{12}$$

where $\Delta x = |x_0 - x_1|$ is the frequency deviation, $\Delta y = |y_1 - y_0|$ is the predicted amplitude change of $y(n)$ responding to Δx, and P_0 is the nominal generated power.

This system contains a total of ten thermal units with joint frequency regulation, as shown in Fig. 6. The dynamic predicted value of primary frequency regulation output can be obtained from Section III-A so that the predicted speed droop ratio can be obtained through calculation.

The self-adjusting system can adjust each unit's droop coefficient by the predicted speed droop ratio to realize the coordination of multiple units for frequency regulation. Typically, numerous units have the same droop coefficient. At 4%–6%, the self-adjusting system adjusts the droop coefficient of each unit according to the predicted status of each unit. Considering the safe operation of thermal power units, the limit value of the speed droop ratio is 4% and 6% when the range is exceeded. The specific strategy is shown in Fig. 6.

The prediction model proposed in Section III obtains the predicted unit output value from the input unit main steam pressure and valve opening degree to obtain the current unit storage status. From the predicted output value, each unit's predicted speed droop ratio is calculated, and this value is input into the self-adjusting system to calculate the actual speed inequality rate of each unit. The primary frequency command P_{Gn} entered in each unit is the product of the actual speed inequality rate and the frequency difference. The input-predicted speed droop ratio is operated in the self-adjusting system, as shown in Fig. 7.

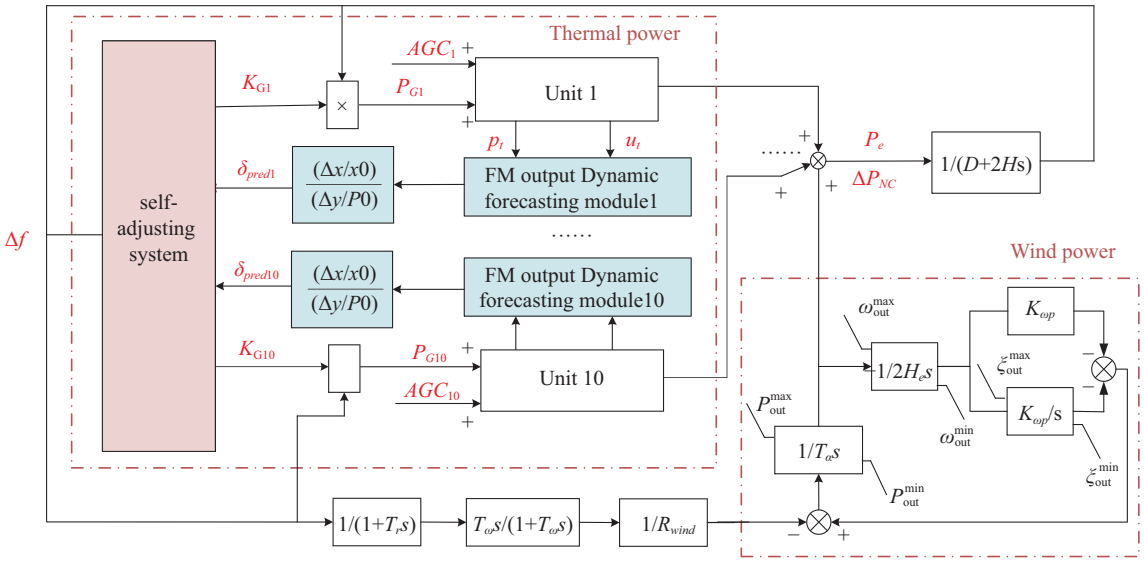

Fig. 6. Improved overall layout of multi-unit combined frequency regulation.

The predicted droop coefficient is obtained according to each unit's predicted speed droop ratio and ranked from largest to smallest to obtain the FRC of each unit. The smaller the predicted droop coefficient is, the worse the PFC capability is. The sum of the predicted droop coefficient and the initial droop coefficient K_{G0} is assigned to each unit from smallest to largest, and the final output K_{Gn}. The self-adjusting system can assign different power factors to different state units to make them respond better to the frequency regulation command.

Among them, the alignment calculation pseudo-code is as follows:

Algorithm 1: Alignment calculation

Input: $K_{\mathrm{pred}n}$ is the Prediction factor n, a_n is the state factor n

Output: K_{Gn} is the Actual Adjustment Factor n

Import $(K_{\mathrm{pred}1}, a_1)$, $(K_{\mathrm{pred}2}, a_2)$, $(K_{\mathrm{pred}3}, a_3)$, $(K_{\mathrm{pred}4}, a_4)$, $(K_{\mathrm{pred}5}, a_5)$, $(K_{\mathrm{pred}6}, a_6)$, $(K_{\mathrm{pred}7}, a_7)$, $(K_{\mathrm{pred}8}, a_8)$, $(K_{\mathrm{pred}9}, a_9)$, $(K_{\mathrm{pred}10}, a_{10})$

$A_i = \mathrm{sorted}(a_n)$

$b_m = A_{11-i}$

$K_{G(11-n)} = -20 + K_{\mathrm{pred}m}$

IV. Validation and Discussion

A. Single Unit Validation

1) Verification and Analysis Under Different Working Conditions

This paper designs a steady-state operating condition for comparison to verify the limited frequency regulation capability of thermal power units under dynamic operating conditions due to insufficient energy storage. The stationary operating point involves completely ignoring the dynamic conditions on the boiler side, with the turbine output power being the standard output power. Under dynamic conditions, considering the boiler-side energy storage brings the output power closer to the actual output. The main steam pressure deviates from the rated value under dynamic conditions, and the simulation is performed by inputting a frequency regulation command at the time of $t = 5$ s for the 60 s. The curve of turbine output power variation under different operating conditions is obtained, as shown in Fig. 8.

The output power of the turbine increases rapidly at the initial moment in both dynamic and steady-state conditions. However, in the dynamic operating conditions, the power drops quickly after about 3 s due to insufficient energy storage. Due to the inertia and delay on the fuel side, the unit energy storage cannot be rapidly increased in the short term, and the extreme value of power output deviation increases with time. However, it can be seen from (a) to (d) that the deviations of the unit's frequency modulation output in dynamic conditions are large compared to the steady-state conditions. The difference in frequency modulation capacity caused by insufficient unit energy storage is close to half of the grid demand at various speed differences. When the speed difference is small, the amount of deviation in the power output when the energy storage is insufficient is also small. The larger the difference, the larger the output deviation will be. It can seem that the unit still has certain responsiveness under the current dynamics in the face of the smaller frequency regulation command. Still, in the face of the large frequency regulation demand, the unit's frequency regulation output under dynamic conditions can hardly meet the grid demand. This also reveals that the larger the frequency difference of the grid, the more difficult it is to complete the frequency regulation process.

B. Prediction Model Accuracy Validation

Based on the theoretical analysis of 3.1–3.2, the main steam flow prediction models and output increment are established. Fig. 9 shows the comparison curves of the predicted and

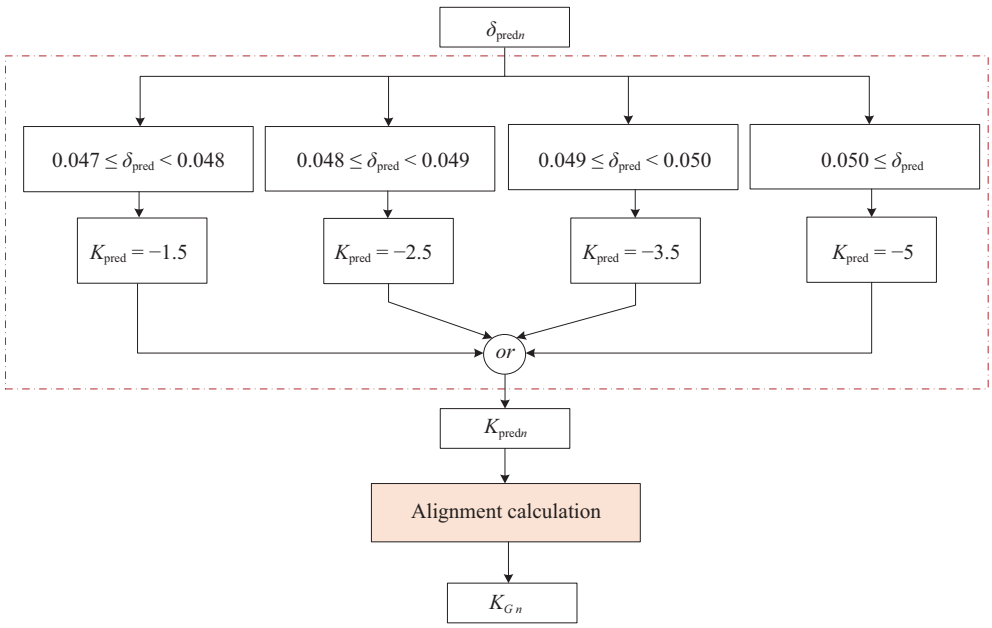

Fig. 7. Self-adjusting system based on predicted speed droop ratio.

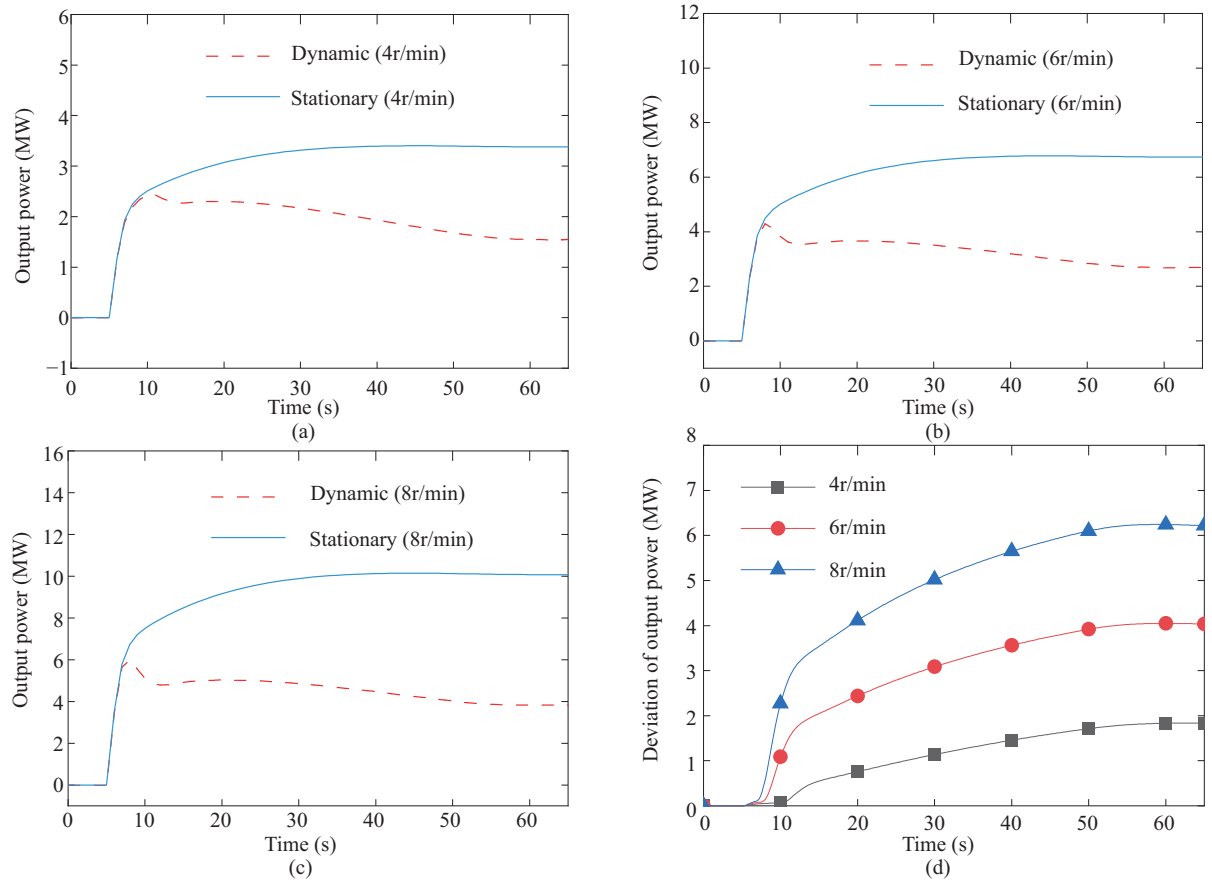

Fig. 8. Output power under different working conditions. (a) 4 rad. (b) 6 rad. (c) 8 rad. (d) Difference value.

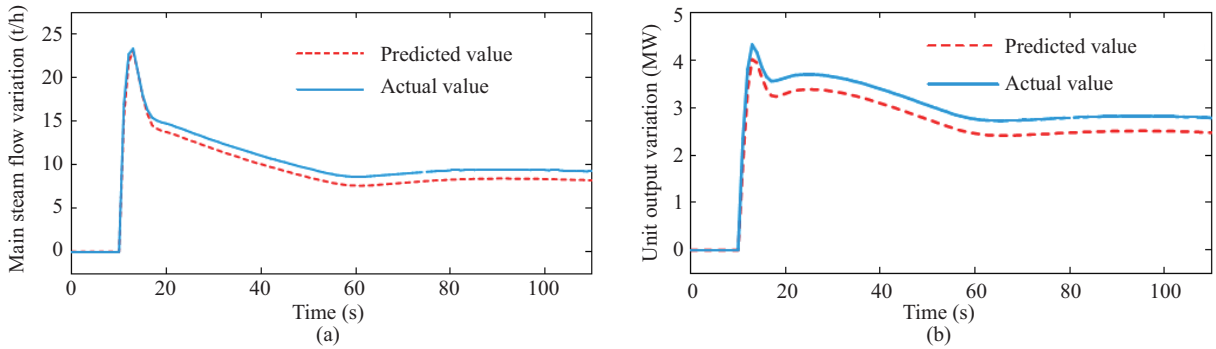

Fig. 9. Predicted curves of main steam flow and unit output power variation. (a) Main steam flow. (b) Unit output power variation.

actual output of main steam flow and turbine frequency output increment under dynamic working conditions after a frequency regulation command is issued. The maximum deviation of the predicted flow rate is 1.48 t/h, which is 0.14% of the rated flow rate, and the maximum deviation of the predicted incremental turbine output is 0.51 MW, which occurs when the frequency regulation command is issued. This has a certain impact on the accuracy of the prediction model. It is known that the correlation coefficients between the predicted and actual output of the main steam flow and the change of the frequency modulation output are 0.9991 and 0.9979, which are higher than 0.99. This comparison shows that the prediction model's result is highly consistent with the actual output in terms of trend. Therefore, the stability of the prediction model under dynamic conditions is verified. The prediction model can meet the design requirements for the coordinated control of the system.

C. Power System Validation

1) System PFC Capability Verification for Different Operating Conditions

The prediction model can evaluate the PFC capacity for the whole system, assuming the same status of ten units. This section presents the experimental results of PFC capability experiments. The PFM load varies from 75%, 50%, 40%, and 30% operating conditions, respectively, to simulate the PFC conditions with speed deviation of 4, 6, and 8 r/min.

TABLE I
EXPERIMENTAL RESULTS OF PFC CAPABILITY

Condition	Speed deviation (rad)	Speed droop ratio(test) (%)	Predicted speed droop ratio (%)	Load(steady)/ Load(target) (%)	Speed droop ratio(test) (%)	Predicted speed droop ratio (%)	Load(steady)/ Load(target) (%)
			75% load			50% load	
Steady-state operating conditions	4	4.967	4.611	92.9	4.976	4.508	91.97
	6	4.977	4.619	92.75	4.984	4.516	91.84
	8	4.986	4.54	92.6	4.993	4.524	91.71
Dynamic working conditions (+10 MW)	4	5.33(No)	4.907	88.53	5.454(No)	4.89	86.71
	6	5.205(No)	4.72	89.72	5.275(No)	4.755	88.31
	8	5.171	4.696	90.02	5.223(No)	4.716	88.77
Dynamic working conditions (−10 MW)	4	4.592	4.298	97.85	4.522	4.138	97.67
	6	4.738	4.333	96.07	4.701	4.281	95.58
	8	4.794	4.377	95.39	4.768	4.334	94.81
			40% load			30% load	
Steady-state operating conditions	4	4.969	4.519	91.57	4.984	4.531	90.97
	6	4.979	4.527	91.44	4.983	4.531	90.95
	8	4.988	4.535	91.32	4.988	4.536	90.88
Dynamic working conditions (+10 MW)	4	5.513(No)	4.923	85.52	5.521(No)	4.935	85.06
	6	5.304(No)	4.78	87.48	6.786(No)	6.104	84.64
	8	5.241(No)	4.738	88.07	8.883(No)	7.971	76.21
Dynamic working conditions (−10 MW)	4	4.478	4.140	97.99	4.519	4.172	96.99
	6	4.675	4.286	95.55	4.69	4.298	94.9
	8	4.747	4.34	94.68	4.753	4.345	9.414

In addition, the dynamic conditions of the system before the onset of primary frequency regulation also significantly impact the PFC capability. The dynamic conditions of load increase (+10 MW) and load reduction (−10 MW) before the primary frequency regulation command's arrival are simulated, and the conclusions are shown in Table I.

Table I shows a great difference between dynamic and steady-state PFC capability under any load, whether $\Delta n =$ 4 rpm, 6 rpm, or 8 rpm, which also proves the necessity of the dynamic prediction model proposed in this paper. When the load is increased before the arrival of the primary frequency regulation command, it means that the unit is in a state of insufficient energy storage, and the integral power index is mainly unable to meet the requirements. When the actual speed ratio of the unit is greater than 5.2, and the PFC capacity is insufficient, the prediction model evaluation result is greater than 4.7. When the load is increased before the arrival of a frequency regulation command, it means that the unit is in a state of sufficient energy storage, and the PFC capacity is better than the steady state. It is easy to see that the smaller the speed deviation, the greater the impact on the PFC capacity when the dynamic situation is under-stored. The opposite is true when energy storage is sufficient. This is in line with our analysis. The PFC capacity of the unit also varies at different loads. When at 75% load, the system has a strong anti-interference ability and frequency modulation effect. When under 30%–50% load, the system has weak anti-interference ability. Especially under 30% load, the speed droop ratio has increased to 6.786 and 8.883 when facing the disturbance of 6 rpm and 8 rpm when the energy storage is insufficient, which is far beyond its reasonable range. Besides, it can be seen from the simulation of multiple cases that the accuracy of the predicted model's speed droop ratio exceeds 90%, and the trend is consistent with the actual results, so it is reasonable to design coordinated control of multiple units.

2) Random State Simulation

The WPP rate α is set to 25%, 50%, and 75%, and the output ratios of conventional units are 75%, 50%, and 25%, respectively. The simulation considers $\Delta n = 4$ rpm under other related parameters shown in Table II.

TABLE II
PARAMETERS OF THE SIMULATION MODEL

λ	T_{HP}	T_{IP}	T_{LP}	F_{HP}	F_{IP}	F_{LP}	M
0.805	0.271	13.562	0.391	0.311	0.253	0.436	2
D	R	T_a	Tr	Tw	Kwp	Kwi	
12	5	0.2	0.1	6	1.68	0.97	

When the unit is in normal condition, the change of frequency difference and system output before and after improvement are shown in Fig. 10. The same color indicates the same WPP, and the state before and after the improvement is distinguished by the line pattern. It can be observed that the maximum deviation gradually increases with the increase in WPP. Although deep peak shaving of power systems preserves system inertia, frequency oscillations increase with increasing WPP. Furthermore, the increased support provided by the WEC does not prevent the frequency performance of the power system from continuously deteriorating with increasing WPP. The maximum frequency deviations improved by 11.7%, 10.5%, and 11.1% when the wind penetration was 25%, 50%, and 75%, respectively. The maximum frequency deviation of the system was reduced after the improvement, regardless of the wind penetration state. Since the dynamic condition of the unit is in a good state, and there is enough energy storage for the response, the unit output is the same at the later stage, and the steady-state frequency deviation is not changed.

When some units of the system are in the under-storage condition, the FRC is reduced. Monte Carlo statistics simulate

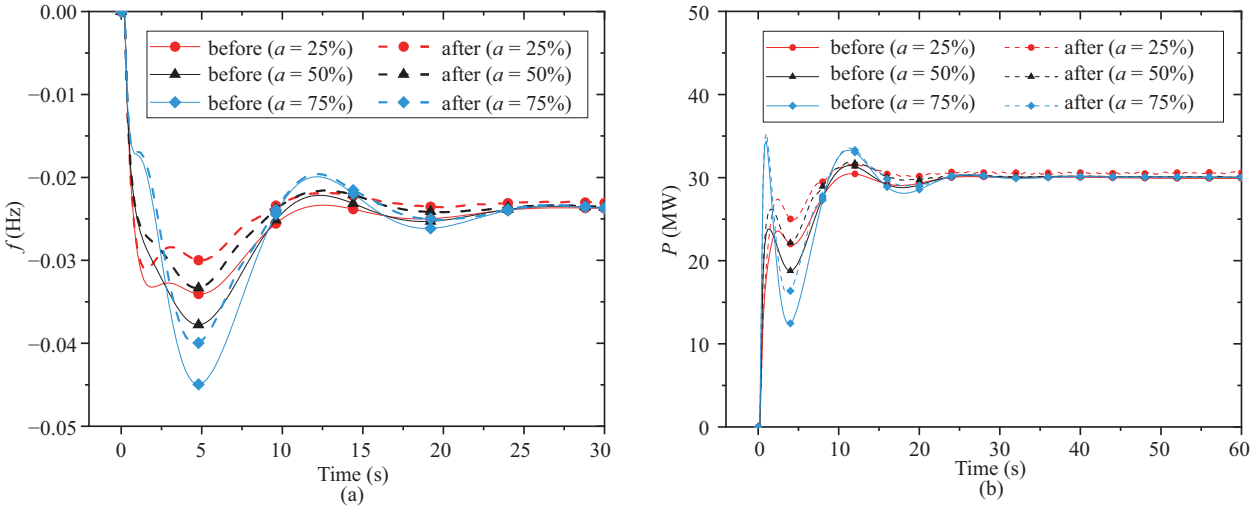

Fig. 10. Frequency difference and output power before and after improvement of different wind power permeability under normal conditions. (a) Frequency comparation. (b) Output power comparation.

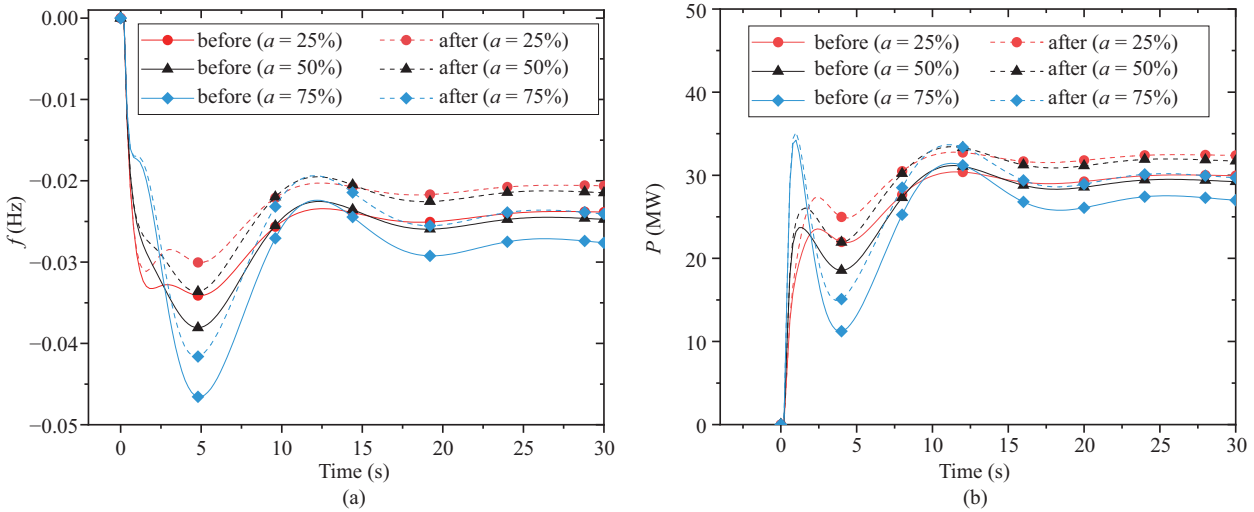

Fig. 11. Frequency difference and output power before and after the improvement of different wind power penetration rates under poor condition. (a) Frequency comparation. (b) Output power comparation.

a typical state worse situation. The change in frequency difference and system output before and after improvement is shown in Fig. 11. The maximum frequency difference before improvement is 0.035, 0.039, and 0.047, respectively. The frequency regulation effect is obviously worse than the state when the energy storage is sufficient. After the improvement, the maximum frequency difference is 0.031, 0.033, and 0.042, which is 11.4%, 15.3%, and 10.6% better than before the improvement. In addition, the proposed strategy can make full use of the energy storage of the unit in good condition to increase the output of the unit, so the steady-state frequency difference is also improved. The improved effect is better than the effect when the condition is good, which proves the effectiveness of the proposed improvement strategy.

The FRC is worst when the units are all in a poor storage state. Insufficient PFC capacity leads to late frequency dropout, which poorly impacts primary frequency regulation. As shown in Fig. 12, the lower the WPP rate, the more serious the frequency drop-off is at the 60 s. This is because when WPP is low, thermal units provide the main FRC. The worse the state of the unit, the greater the impact on the system. The improved maximum frequency difference is increased by 6.7%, 10.4%, and 11.3%.

D. Typical Situation Analysis

Usually, ten units have different response capacities due to different AGC commands. The Monte Carlo statistical idea is used to simulate the distribution of the different energy states of boilers with different units. The dynamic working condition is divided into two cases: load increase and load reduction. The number of units is known to be ten, and the number of simulations is 10, 100, 1 000, and 10 000 times, and the measured state possibilities of the units are shown in Fig. 13.

Where S1 is the worst case of frequency regulation capability, S2 is the worst case, S3 is the normal case, S4 is the better case, and S5 is the best case. The typical normal state,

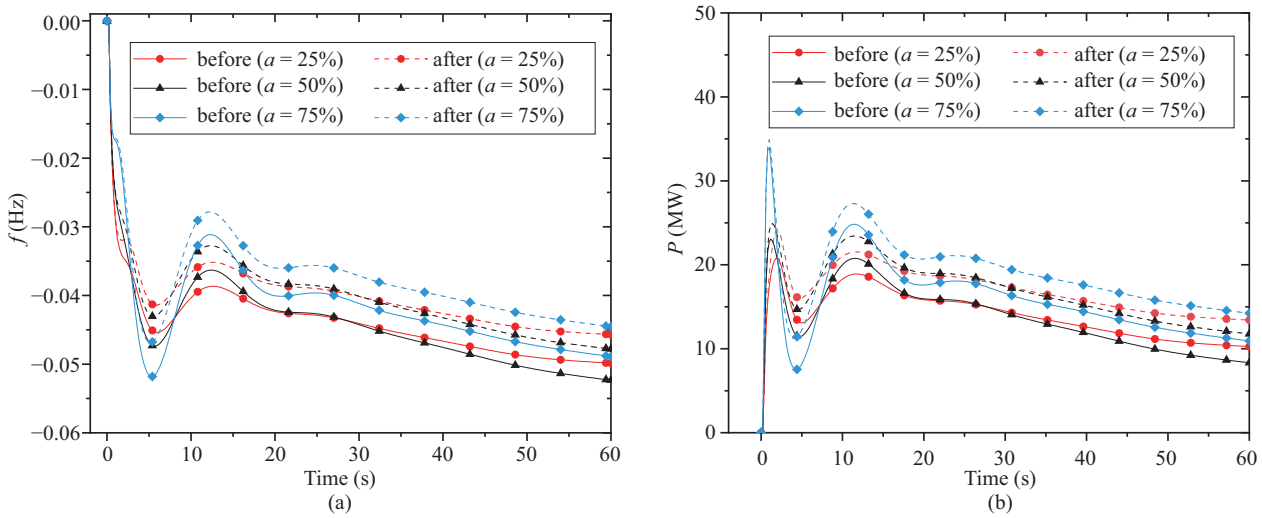

Fig. 12. Frequency difference and output power before and after improvement of different wind power permeability in the worst condition. (a) Frequency comparation. (b) Output power comparation.

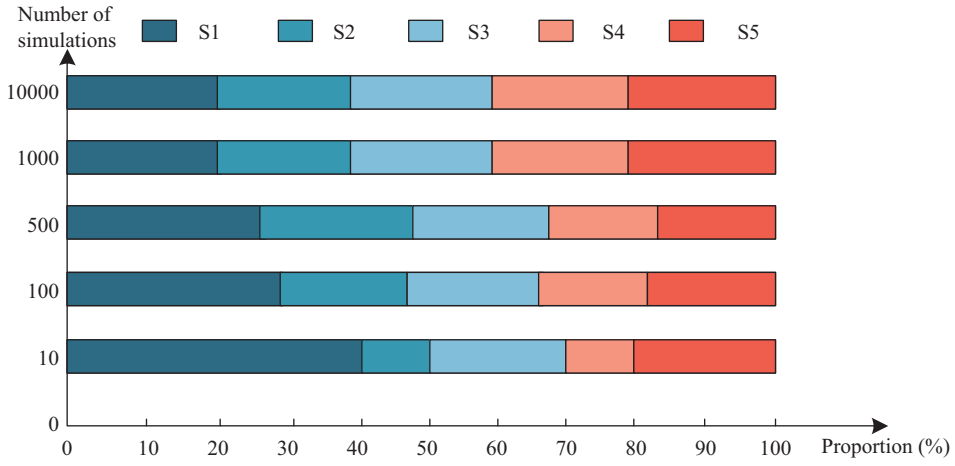

Fig. 13. Monte Carlo statistics.

worst state, and worst state are selected for simulation, and the simulation results are shown in "Random State Simulation" part. From the figure, as the number of simulations increases, the probability of good and bad states appearing is close to 1:1, and the unit's FRC is close to the steady-state regulation capability in a wide range. This situation is consistent with the long-term planning of the unit because the concern is the result of long-term averaging. However, considering the stability of the grid security, the episodic factor must be paid attention to. The smaller the number of simulations, the closer it is to the stochastic probability. When the number of simulations is ten, the unit state appears significantly different, which is then consistent with the unit frequency regulation randomness event. When extreme cases occur, the state of the unit is also insufficient, which proves the necessity of our simulation.

V. Conclusion

In this paper, considering the security and stability of power systems, a dynamic model for frequency evaluation during unit frequency regulation is established based on conventional research with consideration of steam-side energy storage. The correlation coefficients between the predicted and actual output of the variation of main steam flow and the variation of output are 0.9991 and 0.9979, which verify the accuracy of the prediction model.

A modern power system model of flexible thermal power generation containing ten thermal units has been established. The FRC under different wind power penetrations is considered. Based on the dynamically evaluated thermal PFC capability, a multi-unit coordinated flexible, adaptive allocation scheme is proposed. The PFC capability of the system before and after improvement is compared and analyzed through several simulations. Load perturbations are added to the power system model for WPP of 25%, 50%, and 75%, and a significant improvement in the frequency regulation state of the modified units is observed. As the frequency oscillation increases with increasing wind penetration, the maximum frequency difference also changes with it. Simulation results show that the maximum frequency difference is improved by 11.7%, 10.5%, and 11.1% under normal conditions. In typical

poor states, the improvements were 11.4%, 15.3%, and 10.6%, respectively. In the worst conditions, although it could not achieve the effect under the conventional condition, it also achieved an improvement of 6.7%, 10.4%, and 11.3%. The improvement is better at high penetration rates, and the results will help to guide the frequency modulation service.

REFERENCES

[1] K. Q. Sun, H. Q. Xiao, S. T. You, H. Y. Li, J. P. Pan, K. J. Li, and Y. L. Liu, Frequency secure control strategy for power grid with large-scale wind farms through HVDC links, *International Journal of Electrical Power & Energy Systems*, vol. 117, pp. 105706, May 2020.

[2] Z. D. Shi, W. S. Wang, Y. H. Huang, P. Li, and D. Ling, Simultaneous optimization of renewable energy and energy storage capacity with the hierarchical control, *CSEE Journal of Power and Energy Systems*, vol. 8, no. 1, pp. 95–104, Jan. 2022.

[3] J. H. Hao, F. Gao, X. Y. Fang, X. L. Nong, Y. X. Zhang, and F. Hong, Multi-factor decomposition and multi-scenario prediction decoupling analysis of China's carbon emission under dual carbon goal, *Science of the Total Environment*, vol. 841, pp. 156788, Oct. 2022.

[4] Z. Y. Peng, W. S. Lu, and C. J. Webster, Quantifying the embodied carbon saving potential of recycling construction and demolition waste in the Greater Bay Area, China: Status quo and future scenarios, *Science of the Total Environment*, vol. 792, pp. 148427, Oct. 2021.

[5] A. A. Chen, A. J. Stephens, R. Koon Koon, M. Ashtine, and K. Mohammed-Koon Koon, Pathways to climate change mitigation and stable energy by 100% renewable for a small island: Jamaica as an example, *Renewable and Sustainable Energy Reviews*, vol. 121, pp. 109671, Apr. 2020.

[6] J. X. Liu, China's renewable energy law and policy: A critical review, *Renewable and Sustainable Energy Reviews*, vol. 99, pp. 212–219, Jan. 2019.

[7] A. Latif, S. M. Suhail Hussain, D. C. Das, and T. S. Ustun, Double stage controller optimization for load frequency stabilization in hybrid wind-ocean wave energy based maritime microgrid system, *Applied Energy*, vol. 282, pp. 116171, Jan. 2021.

[8] Q. X. Shi, H. T. Cui, F. X. Li, Y. L. Liu, W. Y. Ju, and Y. H. Sun, A hybrid dynamic demand control strategy for power system frequency regulation, *CSEE Journal of Power and Energy Systems*, vol. 3, no. 2, pp. 176–185, Jun. 2017.

[9] B. Xiao et al., "Power Source Flexibility Margin Quantification Method for Multi-Energy Power Systems Based on Blind Number Theory," *CSEE Journal of Power and Energy Systems*, vol. 9, no. 6, pp. 2321–2331, Nov. 2023.

[10] X. J. Li and S. X. Wang, Energy management and operational control methods for grid battery energy storage systems, *CSEE Journal of Power and Energy Systems*, vol. 7, no. 5, pp. 1026–1040, Sep. 2021.

[11] K. Guerra, P. Haro, R. E. Gutirrez, and A. Gmez-Barea, Facing the high share of variable renewable energy in the power system: Flexibility and stability requirements, *Applied Energy*, vol. 310, pp. 118561, Mar. 2022.

[12] Y. L. Liu, L. Mili, Y. Xu, J. B. Zhao, I. Kamwa, D. Srinivasan, A. Mehrizi-Sani, P. Arboleya, and V. Terzijia, Guest editorial: Special issue on data-analytics for stability analysis, control, and situational awareness of power system with high-penetration of renewable energy, *International Journal of Electrical Power & Energy Systems*, vol. 137, pp. 107773, May 2022.

[13] F. Hong, Y. Zhao, W. Ji, F. Fang, J. Hao, Z. Yang, J. Kang, L. Chen, and J. Liu, A feature-state observer and suppression control for generation-side low-frequency oscillation of thermal power units, *Applied Energy*, vol. 354, pp. 122179, Jan. 2024.

[14] D. Al Kez, A. M. Foley, N. McIlwaine, D. John Morrow, B. P. Hayes, M. Alparslan Zehir, L. Mehigan, B. Papari, C. S. Edrington, and M. Baran, A critical evaluation of grid stability and codes, energy storage and smart loads in power systems with wind generation, *Energy*, vol. 205, pp. 117671, Aug. 2020.

[15] S. P. Peng, Current status of national integrated gasification fuel cell projects in China, *International Journal of Coal Science & Technology*, vol. 8, no. 3, pp. 327–334, Jul. 2021.

[16] Y. Bao, J. Xu, S. Y. Liao, Y. Z. Sun, X. Li, Y. Z. Jiang, D. P. Ke, J. Yang, and X. T. Peng, Field verification of frequency control by energy-intensive loads for isolated power systems with high penetration of wind power, *IEEE Transactions on Power Systems*, vol. 33, no. 6, pp. 6098–6108, Nov. 2018.

[17] N. Ding, J. H. Duan, S. Xue, M. Zeng, and J. F. Shen, Overall review of peaking power in China: Status quo, barriers and solutions, *Renewable and Sustainable Energy Reviews*, vol. 42, pp. 503–516, Feb. 2015.

[18] J. J. Wang, S. Zhang, J. K. Huo, Y. Zhou, L. Li, and T. Y. Han, Dispatch optimization of thermal power unit flexibility transformation under the deep peak shaving demand based on invasive weed optimization, *Journal of Cleaner Production*, vol. 315, pp. 128047, Sep. 2021.

[19] J. Hentschel, H. Zindler, and H. Spliethoff, Modelling and transient simulation of a supercritical coal-fired power plant: Dynamic response to extended secondary control power output, *Energy*, vol. 137, pp. 927–940, Oct. 2017.

[20] Y. K. Han, S. Gao, L. Li, W. W. Miao, Y. Y. Li, and Q. Yan, Research on primary frequency modulation of coordinated control system for wind power generator and thermal power unit, *IOP Conference Series: Earth and Environmental Science*, vol. 508, no. 1, pp. 012030, Apr. 2020.

[21] D. Feldmann and R. V. De Oliveira, Operational and control approach for PV power plants to provide inertial response and primary frequency control support to power system black-start, *International Journal of Electrical Power & Energy Systems*, vol. 127, pp. 106645, May 2021.

[22] A. Delavari and I. Kamwa, Improved optimal decentralized load modulation for power system primary frequency regulation, *IEEE Transactions on Power Systems*, vol. 33, no. 1, pp. 1013–1025, Jan. 2018.

[23] G. G. Tu, Y. J. Li, and J. Xiang, Coordinated rotor speed and pitch angle control of wind turbines for accurate and efficient frequency response, *IEEE Transactions on Power Systems*, vol. 37, no. 5, pp. 3566–3576, Sep. 2022.

[24] C. Wu, X. P. Zhang, and M. Sterling, Wind power generation variations and aggregation, *CSEE Journal of Power and Energy Systems*, vol. 8, no. 1, pp. 17–38, Jan. 2022.

[25] H. M. Yang, R. Liang, Y. Yuan, B. W. Chen, S. Xiang, J. P. Liu, H. Zhao, and E. Ackom, Distributionally robust optimal dispatch in the power system with high penetration of wind power based on net load fluctuation data, *Applied Energy*, vol. 313, pp. 118813, May 2022.

[26] M. Huber, D. Dimkova, and T. Hamacher, Integration of wind and solar power in Europe: Assessment of flexibility requirements, *Energy*, vol. 69, pp. 236–246, May 2014.

[27] Y. N. Chi, B. J. Tang, J. B. Hu, X. S. Tian, H. Y. Tang, Y. Li, S. J. Sun, L. Shi, and L. Shuai, Overview of mechanism and mitigation measures on multi-frequency oscillation caused by large-scale integration of wind power, *CSEE Journal of Power and Energy Systems*, vol. 5, no. 4, pp. 433–443, Dec. 2019.

[28] M. D. Xu, H. Yang, W. B. Hao, X. Y. Zhao, and S. Y. Yu, Wind power grid-connected frequency regulation strategy based on ESO control and PI control, *IOP Conference Series: Earth and Environmental Science*, vol. 371, no. 5, pp. 052036, Dec. 2019.

[29] J. Yao, M. T. Yu, W. Z. Gao, and X. Zeng, Frequency regulation control strategy for PMSG wind-power generation system with flywheel energy storage unit, *IET Renewable Power Generation*, vol. 11, no. 8, pp. 1082–1093, Jun. 2017.

[30] A. Abazari, H. Monsef, and B. Wu, Load frequency control by de-loaded wind farm using the optimal fuzzy-based PID droop controller, *IET Renewable Power Generation*, vol. 13, no. 1, pp. 180–190, Jan. 2019.

[31] A. Abazari, H. Monsef, and B. Wu, Coordination strategies of distributed energy resources including FESS, DEG, FC and WTG in load frequency control (LFC) scheme of hybrid isolated micro-grid, *International Journal of Electrical Power & Energy Systems*, vol. 109, pp. 535–547, Jul. 2019.

[32] S. Q. Wang and K. Tomsovic, Fast frequency support from wind turbine generators with auxiliary dynamic demand control, *IEEE Transactions on Power Systems*, vol. 34, no. 5, pp. 3340–3348, Sep. 2019.

[33] Q. L. Tan, Y. H. Ding, J. Zheng, M. Dai, and Y. M. Zhang, The effects of carbon emissions trading and renewable portfolio standards on the integrated wind–photovoltaic–thermal power-dispatching system: Real case studies in China, *Energy*, vol. 222, pp. 119927, May 2021.

[34] S. J. Li, Q. S. Xu, Y. X. Xia, and K. Hua, Comprehensive setting and optimization of dead-band for BESS participate in power grid primary frequency regulation, *International Journal of Electrical Power & Energy Systems*, vol. 141, pp. 108195, Oct. 2022.

[35] M. Garcia and R. Baldick, Requirements for interdependent reserve types providing primary frequency control, *IEEE Transactions on Power Systems*, vol. 37, no. 1, pp. 51–64, Jan. 2022.

[36] M. Zeng, X. M. Liu, and L. L. Peng, The ancillary services in China: An overview and key issues, *Renewable and Sustainable Energy Reviews*, vol. 36, pp. 83–90, Aug. 2014.

[37] P. J. C. Vogler-Finck and W. G. Frh, Evolution of primary frequency control requirements in Great Britain with increasing wind generation,

International Journal of Electrical Power & Energy Systems, vol. 73, pp. 377–388, Dec. 2015.
[38] L. Gao, Y. P. Dai, J. F. Wang, P. Zhao, and T. Zhao, An online estimation method of primary frequency regulation parameters of generation units, *Proceedings of the CSEE*, vol. 32, no. 16, pp. 62–69, Jun. 2012.
[39] J. L. Liao, Primary frequency control ability Modeling and optimization of large-scale thermal power units, Ph.D. dissertation, Zhejiang University, Hangzhou, 2020.
[40] D. L. Zeng, Y. K. Gao, Y. Hu, and J. Z. Liu, Optimized control of the drum boiler power plant's coordination system based on stair-like generalized predictive control, *Proceedings of the CSEE*, vol. 39, no. 16, pp. 4819–4826, Aug. 2019.
[41] Y. M. Tang, Y. Bai, C. Z. Huang, and B. Du, Linear active disturbance rejection-based load frequency control concerning high penetration of wind energy, *Energy Conversion and Management*, vol. 95, pp. 259–271, May 2015.
[42] F. Hong, W. Ji, Y. Pang, J. Hao, M. Du, F. Fang, and J. Liu, A new energy state-based modeling and performance assessment method for primary frequency control of thermal power plants, *Energy*, vol. 276, pp. 127594, Aug. 2023.

Feng Hong received the Ph.D. degree in Control Theory and Control Engineering from North China Electric Power University, Beijing, China, in 2019. He is currently a Lecturer with the School of Control and Computer Engineering, North China Electric Power University. His current research interests include renewable energy integration and flexibility of the power generations.

Yalei Pang is an M.S. student in Control Engineering at North China Electric Power University, Beijing, China. Her research topics are focused on energy storage and power generation combined to support grid frequency modulation control.

Weiming Ji a Ph.D. student, is working at School of Control Science and Engineering, North China Electric Power University. His research topics are focused on thermal power plant modeling and optimal regulation.

Lu Liang received the B.S. degree in Control Engineering from North China Electric Power University, Beijing, China, in 2019. He is currently working toward the M.S. degree in Control Engineering at North China Electric Power University, Beijing, China. His main research interest is energy storage assisted frequency modulation control.

Fang Fang received the Ph.D. degree in Thermal Power Engineering from North China Electric Power University, Beijing, China, in 2005. He is currently a Professor of Control Science and Engineering and the Dean of the School of Control and Computer Engineering with North China Electric Power University. His current research interests include forecasting of integrated energy systems and intelligent power generation technologies.

Junhong Hao received the Ph.D. degree in Engineering Mechanics from Tsinghua University, Beijing, China, in 2017. He is currently an Associate Professor of School of Energy Power and Mechanical Engineering, North China Electric Power University. His research interests are mainly in Energy storage technology and integrated energy system optimization.

Jizhen Liu received the M.S. degree in Power Plant Engineering from the Graduate Faculty of North China Electric Power Institute, Beijing, China, in 1982. He is now an Academician of Chinese Academy of Engineering, and a Professor with the State Key Laboratory of Alternate Electrical Power System with Renewable Energy Sources, North China Electric Power University. His research interests include new power system power generation.